Europhys. Lett., **40** (5), pp. 569-574 (1997)

The non-resonant magnetic X-ray scattering cross-section for photon energies up to 500 keV

J. Strempfer[1], Th. Brückel[1](*), D. Hupfeld[1], J. R. Schneider[1]
K.-D. Liss[2], and Th. Tschentscher[2]

[1] *Hamburger Synchrotronstrahlungslabor HASYLAB*
at Deutsches Elektronen-Synchrotron DESY
Notkestr. 85, D-22607 Hamburg, Germany
[2] *European Synchrotron Radiation Facility ESRF*
BP 220, F-38043 Grenoble Cedex, France

(received 4 September 1997; accepted 20 October 1997)

PACS. 75.25+z – Spin arrangements in magnetically ordered materials (including neutron and spin-polarized electron studies, synchrotron-source X-ray scattering, etc.).
PACS. 78.70Ck – X-ray scattering.

Abstract. – Results of high-energy magnetic X-ray diffraction for photon energies up to 500 keV are presented and the form of the magnetic scattering cross-section for relativistic energies is discussed. At 300 keV we experimentally proved that the scattering from the spin component perpendicular to the scattering plane is dominant. Within our statistical and systematic errors, the magnetic scattering amplitude for this component does not exhibit any variation with energy between 100 and 500 keV.

Introduction. – Magnetic X-ray diffraction with high-energy photons exhibits certain advantages with respect to neutron and medium-energy X-ray diffraction which are discussed in detail in [1], [2]. These include true bulk sensitivity, volume-enhancement of the magnetic signal, high momentum space resolution and a simple form of the magnetic scattering cross-section. For this reason, magnetic scattering with hard X-rays at an energy of 80 keV has been developed during the last years [1], [2]. At this energy, the first-order approximation in $\hbar\omega/mc^2$ for the magnetic scattering amplitude is valid in very good approximation. For magnetic diffraction at higher energies, when the photon energy approaches the electron rest mass $mc^2 = 511$ keV, a complete quantum-relativistic treatment is necessary, taking into account all effects arising from the coupling of the quantized photon field and the Dirac field of the electrons. To our knowledge, a corresponding theory is missing.

To investigate experimentally how the scattering cross-section behaves for higher photon energies, we measured magnetic Bragg reflections of MnF_2 at energies up to 500 keV.

Magnetic scattering cross-section for hard X-rays. – A calculation of the cross-section for X-ray scattering including the magnetic terms from a quasi-relativistic Hamiltonian for

(*) Present address: Forschungszentrum Jülich, Institut für Streumethoden, D-52425 Jülich, Germany.

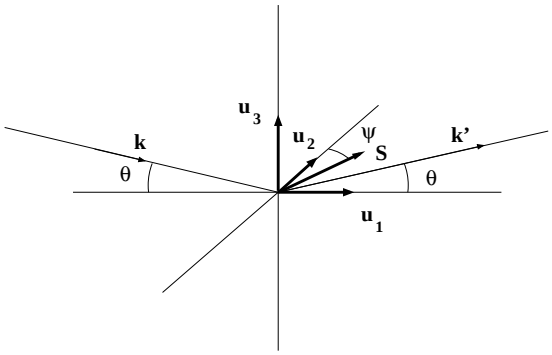

Fig. 1

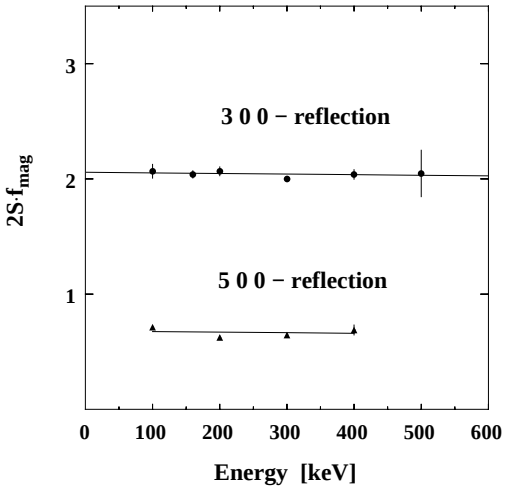

Fig. 2

Fig. 1. – Definition of the basis vectors $\mathbf{u}_i$ for the magnetic structure. $\mathbf{k}$ and $\mathbf{k}'$ are the incident and scattered wavevectors and Ψ is the angle between $\mathbf{u}_2$ and the spin moment in the ($\mathbf{u}_2$, $\mathbf{u}_1$)-plane.

Fig. 2. – Energy dependence of the magnetic structure factor from 100 keV to 500 keV. The solid lines represent the fits to the data. Shown are the statistical errors only. The systematic errors are detailed in table I.

electrons in a quantized electromagnetic field within second-order perturbation theory was done by Blume [3] and Blume and Gibbs [4]. Platzman and Tzoar [5] and de Bergevin and Brunel [6] started from the Dirac equation and reduced this relativistic ansatz using a Foldy-Wouthuysen transformation to a quasi–non-relativistic form analogous to that obtained from the non-relativistic Hamiltonian. The expansion of this quasi–non-relativistic Hamiltonian in dependence of photon energy over electron rest mass $\hbar\omega/mc^2$ allows the description of the magnetic scattering process. Grotch, Kazes, Bhatt and Owen [7] extended the Foldy-Wouthuysen transformation to second order in $\hbar\omega/mc^2$. The dominating contribution to pure magnetic scattering is given by the first-order term. While the second-order term is sensitive to charge scattering only, the next magnetic contribution in the expansion is expected from the third-order term. The strongest magnetic contribution stems from the first-order term and its interference term with charge scattering. The next strongest magnetic contribution arises from the interference term between charge scattering and the third-order magnetic scattering. Since the contribution of these interference terms is difficult to investigate for antiferromagnets, we will focus on the pure magnetic contributions. The next pure magnetic contribution to the scattering amplitude is expected to be of third-order.

For photon energies of $\hbar\omega \leq 100$ keV these higher-order terms are negligible [1]. In contrast to Compton scattering [8], [9], for magnetic Bragg diffraction kinematic factors exist which cancel the energy dependence of the cross-section. Thus, the resulting magnetic scattering cross-section for an intermediate energy range of $\hbar\omega \leq 100$ keV reduces to

$$\left(\frac{\mathrm{d}\sigma}{\mathrm{d}\Omega}\right)_{\mathrm{magnetic}} = r_0^2 \left(\frac{\lambda_{\mathrm{C}}}{d}\right)^2 |S_2|^2 \,. \tag{1}$$

Here, r_0 is the classical electron radius, λ_{C} the Compton wavelength, d the inter-planar lattice spacing of the magnetic reflection and S_2 the spin component perpendicular to the scattering

plane (see fig. 1). For energies close to $\hbar\omega = 511\,\mathrm{keV}$, each matrix element of the Hamiltonian has to be evaluated separately [7]. This has not been done until now.

Experimental. – The experiment was conducted at the beamline ID15A at ESRF, using the superconducting wavelength shifter with a critical energy of 100 keV at a magnetic field of 4 T. The crystal was mounted in an ILL-type Orange He-Cryostat.

Two different MnF_2 crystals have been used. For the energy-dependent measurements it was a 2 mm thick platelet with lateral dimensions of $10 \times 15\ \mathrm{mm}^2$ with an a-axis normal to the plate. For the rotation of the spin direction into the scattering plane we used a crystal with dimensions $5.9 \times 5.9 \times 6.1\ \mathrm{mm}^3$.

MnF_2 is a uniaxial antiferromagnet where the spins are aligned in the $\pm\mathbf{c}$-direction. Due to the crystal symmetry detailed in [10], charge reflections are forbidden at positions $h\,0\,0$ with h odd. At these positions, pure magnetic scattering can be observed.

The experiment was done in two crystal mode without an analyzer. We used an annealed Si-3 1 1 crystal with a rocking curve width of about $6''$ at 100 keV as monochromator.

Results. – At 100, 160, 200, 300, 400 and 500 keV, we measured magnetic reflections of type $h\,0\,0$ with h odd. Multiple scattering was significant at an energy of 100 keV. However, as simulated in [2], multiple scattering does not pose a problem for higher energies. Due to the large Ewald sphere regions without multiple scattering can be found by rotation of the crystal around the scattering vector. The count rates of the magnetic 3 0 0 reflection varied from 3600 counts/s at 100 keV to 2 counts/s at 500 keV. To measure the energy dependence of magnetic Bragg scattering, the magnetic intensities have to be measured on an absolute scale. This can be done either by a measurement of the incident flux via a Compton experiment [11] or by relating the magnetic intensities to the intensities of charge reflections. Here we choose the latter method, since all absorption effects due to sample environment and detector windows cancel out and can be neglected. A similar argument holds for the energy dependence of quantum efficiency of the Ge detector. For the normalization procedure we measured the charge reflections which occur at positions $h\,0\,0$ with h even. Since charge reflections can only be measured with thick attenuators, a calibration of the Fe filters had to be done for each energy. We measured the same reflection with several filters covering the whole dynamical range of the Ge detector. In order to obtain the absorption coefficient, we fitted the dependence of the integrated intensities on the attenuator thickness with an exponential function. This method turned out to be very sensitive to the dead time correction since very high count rates are involved. The best fit of the exponential was achieved with a dead time of $\tau = 3\,\mu\mathrm{s}$.

The primary intensity was calculated from the charge reflections using the scattering factors from International Tables for Crystallography [12] and lattice constants and Debye-Waller factors from Jauch *et al.* [13]. At 100 keV extinction was considerable. The strongest effect was of order of 30%, which could be corrected for by application of the Zachariasen model assuming a type-I crystal, which is expected for the small wavelengths [14]. At higher energies extinction becomes less and less pronounced. Despite the very narrow rocking curve width of 6.5 in., we consider only secondary extinction, since at these energies the extinction length is of order $t_{\mathrm{ext}} = 0.1$–0.3 mm and the size of the mosaic blocks is much smaller (the Darwin width is 0.3 in. to 0.05 in. depending on the energy).

For a comparison of charge and magnetic reflections, the absorption of the sample is nearly negligible, because of the very small variations of the diffraction angles. The magnetic structure factor is calculated as follows:

$$(F_{\mathrm{m}})^2 = \frac{I_{\mathrm{m}}}{I_{\mathrm{c}}} \left(\frac{d}{\lambda_{\mathrm{C}}}\right)^2 \frac{\sin\theta_{\mathrm{B}}^{\mathrm{m}}}{\sin\theta_{\mathrm{B}}^{\mathrm{c}}} (F_{\mathrm{c}})^2 \left(\frac{W_{\mathrm{c}}}{W_{\mathrm{m}}}\right)^2 \frac{T_{\mathrm{c}}}{T_{\mathrm{m}}}\ y_{\mathrm{ext}}, \tag{2}$$

TABLE I. – *Magnetic structure factors measured at photon enegies from* 100 KeV *to* 500 KeV.

Reflection	Energy (keV)	magnetic structure factor	statistical error	systematic error
1 0 0	200	4.55	±0.08	$^{+0.29}_{-0.20}$
3 0 0	100	2.07	±0.06	$^{+0.26}_{-0.22}$
	160	2.04	±0.03	$^{+0.18}_{-0.14}$
	200	2.07	±0.04	$^{+0.13}_{-0.09}$
	300	2.00	±0.02	$^{+0.12}_{-0.13}$
	400	2.04	±0.04	$^{+0.01}_{-0.10}$
	500	2.05	±0.20	$^{+0.11}_{-0.08}$
5 0 0	100	0.71	±0.01	$^{+0.09}_{-0.08}$
	200	0.62	±0.01	$^{+0.04}_{-0.04}$
	300	0.64	±0.01	$^{+0.04}_{-0.04}$
	400	0.69	±0.04	$^{+0.04}_{-0.02}$

where I_{m} is the integrated magnetic intensity, I_{c} the integrated intensity of the charge reflections corrected for Fe filters, and $\theta_{\mathrm{B}}^{\mathrm{m}}$ and $\theta_{\mathrm{B}}^{\mathrm{c}}$ are the Bragg angles of the charge and the magnetic reflection, respectively. F_{c} is the structure factor for the charge reflection and y_{ext} the corresponding extinction coefficient. W_{c} and W_{m} are the Debye-Waller factors, and T_{c} and T_{m} the transmission factors for the charge and magnetic reflections, respectively. The magnetic structure factors for the 3 0 0 and 5 0 0 reflections are shown in fig. 2 as a function of the photon energy.

In table I, the systematic errors are tabulated in addition to the statistical errors. The systematic errors involve the uncertainty of the appropriate extinction model, the dead time correction and the error arising from the normalization to different charge reflections.

At 200 keV, the magnetic structure factor dependence has been measured with reflections 1 0 0, 3 0 0 and 5 0 0. As shown in fig. 3, the experimental data are in good agreement with the structure factor for Mn^{2+} taken from [15], taking into account both statistical and systematic error.

In addition to the energy dependence of the magnetic structure factor, we measured the magnetically scattered intensities for the spin $\mathbf{S}$ lying in all three directions $\mathbf{u}_1$, $\mathbf{u}_2$ and $\mathbf{u}_3$ (compare fig. 1). For measurement with $\mathbf{S} \,||\, \mathbf{u}_2$ and $\mathbf{S} \,||\, \mathbf{u}_1$, we used the 3 0 0 reflection, whereas for $\mathbf{S} \,||\, \mathbf{u}_3$, we used the 0 0 3 reflection. As predicted by eq. (1), we could only observe intensity for $\mathbf{S} \,||\, \mathbf{u}_2$ that means $\mathbf{S}$ perpendicular to the scattering plane. Taking into account the statistics of the scans performed with $\mathbf{S}$ lying in the scattering plane, we can estimate the components in the scattering cross-section with $\mathbf{S} \,||\, \mathbf{u}_3$ and $\mathbf{S} \,||\, \mathbf{u}_1$ to be not larger than 2% and 4% of that with $\mathbf{S} \,||\, \mathbf{u}_2$, respectively. We also turned the crystal around the scattering vector (Ψ rotation)

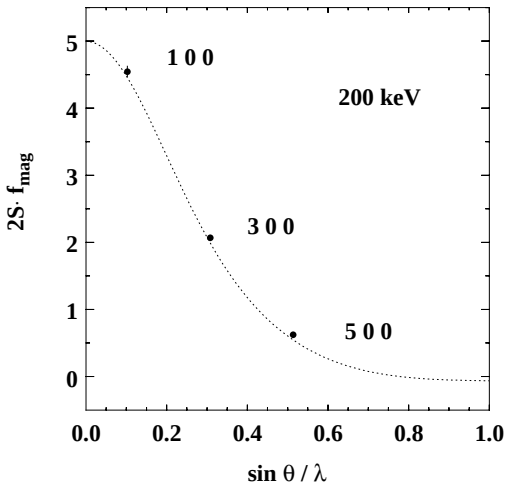

Fig. 3

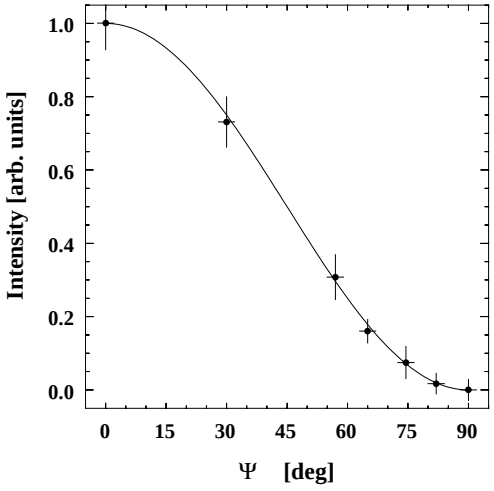

Fig. 4

Fig. 3. – Magnetic structure factor measured at 200 keV photon energy. The dashed line represents the magnetic structure factor calculated with the magnetic form factor for Mn^{2+}.

Fig. 4. – Dependence of the intensity of the magnetic 3 0 0 reflection as a function of Ψ. The crystal is rotated around the scattering vector from $\mathbf{S} \,||\, \mathbf{u}_2$ to $\mathbf{S} \,||\, \mathbf{u}_1$. The solid line represents the behavior predicted by eq. (1). The intensity for $\mathbf{S} \,||\, \mathbf{u}_2$ is normalized to one.

from $\mathbf{S} \,||\, \mathbf{u}_2$ to $\mathbf{S} \,||\, \mathbf{u}_1$ in steps of 7° to 30°. The intensity measured for the different angles in Ψ from 0° to 90°, shown in fig. 4, is exactly described by eq. (1). The uncertainty in Ψ stems from the fact that for each 30° position in Ψ, the sample had to be remounted, since our cryostat allowed only a movement in Ψ of ±8°.

Discussion. – Our experimental results show that the "medium energy" approximation eq. (1) for the magnetic scattering cross-section holds even at photon energies close to the energy equivalent of the rest mass of the electron. This is in clear contrast to magnetic Compton scattering, where the cross-section increases with photon energy [8], [9]. The reason is that for elastic magnetic scattering at different photon energies the momentum transfer stays constant, leading to a kinematical factor which cancels the $\hbar\omega/mc^2$ dependence. We have to emphasize that our present results are restricted to a pure spin system and to pure magnetic scattering. No conclusions can be drawn with respect to the contribution of an orbital angular momentum, but as eq. (1) shows, scattering from orbital angular momentum is already negligible at "medium high" energies around 80 keV. Also the investigation of the energy dependence of interference scattering at mixed charge-magnetic reflections remains a separate task.

Summary. – In our study of the energy dependence of magnetic diffraction, we were able to measure magnetic Bragg reflections up to a photon energy of 500 keV, and to deduce the magnetic structure factor. We can conclude that there is no remarkable contribution of higher-order terms to the magnetic scattering cross-section for energies larger than 100 keV. Also possible contributions of spin components S_1 and S_3 must be smaller than 4% and 2% of the first-order term of the scattering cross-section, respectively. The full relativistic calculation of the scattering cross-section to show the precise dependence on photon energy has still to be done.

***

We would like to thank W. JAUCH and J. BARUCHEL for providing the MnF_2 sample crystals. This work was supported by the BMBF under contract number 03-BR4DES-2 and by the EG human mobility and capital network CHRX-CT930135.

REFERENCES

[1] LIPPERT M., BRÜCKEL TH., KÖHLER TH. and SCHNEIDER J. R., *Europhys. Lett.*, **27** (1994) 537.
[2] STREMPFER J., BRÜCKEL TH., RÜTT U., SCHNEIDER J. R., LISS K.-D. and TSCHENTSCHER TH., *Acta Crystallogr. A*, **52** (1996) 438.
[3] BLUME M., *J. Appl. Phys.*, **57** (1985) 3615.
[4] BLUME M. and GIBBS D., *Phys. Rev. B*, **37** (1988) 1779.
[5] PLATZMAN P. M. and TZOAR N., *Phys. Rev. B*, **2** (1970) 3556.
[6] DE BERGEVIN F. and BRUNEL M., *Acta Crystallogr. A*, **37** (1981) 314.
[7] GROTCH H., KAZES E., BHATT G. and OWEN D. A., *Phys. Rev. A*, **27** (1983) 243.
[8] MCCARTHY J. E., COOPER M. J., HONKIMÄKI V., TSCHENTSCHER TH., SUORTTI P., GARDELIS S., HÄMÄLÄINEN K., MANNINEN S. and TIMMS D. N., to be published in *Nucl. Instrum. Methods A*.
[9] SAKAI N., *J. Appl. Crystalllogr.*, **29** (1996) 81.
[10] BRÜCKEL TH., LIPPERT M., KÖHLER TH., SCHNEIDER J. R., RILLING V., SCHILLING M. and PRANDL W., *Acta Crystallogr. A*, **52** (1996) 427.
[11] STREMPFER J., BRÜCKEL TH., HUPFELD D. and SCHNEIDER J. R., *HASYLAB Jahresbericht*, (1996) 636.
[12] MASLEN E. N., FOX A. G. and O'KEEFE M. A., *International Tables for Crystallography*, Vol. C (Kluwer Academic Publishers) 1992, pp. 476-511.
[13] JAUCH W., SCHULTZ A. J. and SCHNEIDER J. R., *J. Appl. Crystallogr.*, **21** (1988) 975.
[14] ZACHARIASEN W. H., *Acta Crystallogr.*, **23** (1967) 558.
[15] BROWN P. J., *International Tables for Crystallography*, Vol. C (Kluwer Academic Publishers) 1992, pp. 391-399.